Creep behaviour of injection-moulded basalt fibre reinforced poly(lactic acid) composites

Tábi Tamás, Bakonyi Péter, Hajba Sándor, Pedro Jesus Herrera Franco, Czigány Tibor, Kovács József Gábor

TITLE:

Creep behaviour of injection moulded basalt fibres reinforced Poly(Lactic Acid) composites

AUTHORS:

T. Tábi*[1,2], P. Bakonyi[2], S. Hajba[2], P. J. Herrera-Franco[3], T. Czigány[1,2], J. G. Kovács[2]

[1]MTA–BME Research Group for Composite Science and Technology, Muegyetem rkp. 3., H-1111 Budapest, Hungary, corresponding author, tabi@pt.bme.hu, tel.: +36 (1) 463-14-59, Fax: +36 (1) 463-15-27

[2]Department of Polymer Engineering, Faculty of Mechanical Engineering, Budapest University of Technology and Economics, Muegyetem rkp. 3., H-1111 Budapest, Hungary, kovacs@pt.bme.hu

[3]Yucatan Centre for Scientific Research (CICY), Calle 43 #.130, Col. Chuburná de Hidalgo, C.P. 97200 Mérida, Yucatán, Mexico

Abstract

In this paper the creep of short (chopped) basalt fibre reinforced Poly(Lactic Acid) (PLA) composites was investigated. 5, 10, 20 and 30wt% short basalt fibre reinforced composites were prepared by using twin-screw extrusion followed by injection moulding. Differential Scanning Calorimetry (DSC) measurements revealed that the basalt fibres had nucleating effect on the PLA grade used in this study, while Scanning Electron Microscopy (SEM) demonstrated that there was strong adhesion between the fibre and the matrix. Fibre distribution analysis showed that there was no significant statistical difference between the average fibre lengths of all of the produced composites. Finally, creep mastercurves were constructed using the single creep curves obtained by applying 10, 20, 30, …, 90% of the tensile strength of the composites as a static creep loading force. It was demonstrated that the basalt fibres as reinforcements can effectively reduce the strain and increase time to failure of the composites during creep load and thus could open the possibilities for PLA based composites to be used in long-term constantly loaded structural or engineering applications.

1. Introduction

Nowadays, there is a growing interest in the application of biodegradable polymers due to environmental consciousness. Since some members of the biodegradable polymers are also renewable resource based they are believed to solve or at least to moderate the petrol dependency of the plastic industry as well as the waste management problems caused by accumulation of non-biodegradable, low life-cycle plastic products mostly coming from the packaging industry.[1]

Currently, the most promising biodegradable polymer is the starch and sugar based Poly(Lactic Acid) (PLA),[2] which is already commercialized as bottles, cups, cutleries, office utensils, agricultural mulch films, medical bio-absorbable implants, etc., and actively researched to widen its applications for instance by foaming,[3] by increasing biodegradation rate[4] or having shape-memory properties.[5] PLA is a semi-crystalline aliphatic thermoplastic polyester with high strength (tensile strength around 60-65 MPa), high stiffness (tensile modulus around 3-3.5 GPa) but with rather low impact strength (Charpy notched and unnotched impact strength around 2.7 and 23 kJ/m^2 respectively) and heat deflection temperature (HDT) of around 50-55°C. To overcome these drawbacks of low impact strength and HDT, reinforcing fibres are typically introduced to PLA to prepare composites.[6] In most cases plant fibres and thus renewable resource based fibres are used for composite preparation; in this way the final composite is mostly referred to as biocomposite.[7-17] Unfortunately, plant fibres also have some major drawbacks compared to synthetic fibres of glass or carbon, like the higher deviation of the properties of the fibres, which is influenced by the source of the fibre, the age of the plant and the fibre extraction method used. Further drawbacks are the significant water uptake, lower mechanical properties compared to synthetic fibres, and the susceptibility to thermal degradation.[18] Accordingly, the biocomposites with higher mechanical properties are often achieved with pulltrusion[10] or film stacking[11,12] methods to keep the extent of degradation of the fibres low and the fibre ratio as well as the length of the fibres ratio high. At the same time, the high cycle time method of film-stacking is not always suitable to commercialize PLA biocomposite products in an economic way,

moreover, only flat-like products could be made this way. Subsequently, injection moulding can be used to preferably produce complex 3D shaped parts with low cycle time in an economic way, making this processing technology the most feasible to commercialize PLA products. However, there are only minor or moderate improvements in the mechanical properties of the biocomposites when injection moulding is applied[13,14] due to the thermal degradation of the fibres as well as fibre breakage, that resulted in a low fibre aspect ratio (around 40-50%) and finally due to the lower design-ability of the mechanical properties caused by the partial in-flow fibres orientation, since only a shell layer contains in-flow oriented fibres, while the core layer contains fibres with random orientation. As it is demonstrated, it is challenging to produce injection moulded biocomposites with high mechanical properties mainly due to the properties of the plant fibres and also due to some features of the injection moulding technology.

An alternative to plant fibres could be a rather new reinforcing material, the basalt fibres.[19-21] Although basalt fibres are not plant and thus not renewable resource based, but mineral fibres, they are still considered as natural like the plant fibres since basalt can be found in the nature in the form of basalt rocks virtually all over the Globe. Moreover, it is a biologically and chemically inert material and by the weathering of basalt rocks, it increases the mineral content of soil, which features also increase the natural character of basalt. By simply melting the basalt rocks, short or continuous basalt fibres can be made by using the spinneret or the Junkers technology respectively.[22] Although basalt seems to be a good alternative to plant fibres, there are only a limited number of publications in the literature of basalt fibre reinforced PLA based composites[23-27] or basalt fibre reinforced other biodegradable matrix composites like starch[28] or gluten.[29] Xi et al.[23] produced PLA based scaffolds for hard tissue repair with basalt fibre reinforcement. It was proved that the basalt fibres significantly reduce the rate of degradation of the scaffold, and also decreases inflammatory responses caused by acidification during absorption of the PLA. It was confirmed that PLA scaffolds reinforced with basalt fibres can be potentially used in hard tissue repair. It was proved by Liu et al.[24] that basalt fibres with certain sizing can significantly increase tensile, bending and impact

strength of PLA. It was possible to further increase the impact strength of PLA from 19 kJ/m^2 to 34 kJ/m^2 (unnotched impact strength) at 20wt% of basalt fibre content by adding 20wt% of ethylene-acrylate-glycidyl methacrylate copolymer (EAGMA) to the composite. Kurniawan et al.[25] analysed the adhesion between surface treated (atmospheric pressure glow discharge plasma polymerization) basalt fibres and PLA. It was proved that by increasing the plasma polymerisation time above 3 minutes, the tensile strength of the composites increased above the own strength of PLA. The plasma polymerised fibres were well wetted by the PLA as demonstrated by using electron microscopy, however the tensile strength of the composite was lower compared to results from Liu et al.[24] In our previous publication[26] related to injection moulded PLA reinforced with short (chopped) basalt fibres it was demonstrated that it is possible to develop strong adhesion between the PLA and the basalt fibres by using silane sizing. The strong adhesion was demonstrated by electron microscopy by observing excellent wetting of the fibres. Recently, in our other publication,[27] long basalt fibre reinforced injection moulded PLA composites were prepared by first producing a pre-product of basalt roving extrusion coated with PLA and followed by injection moulding of this pre-product. It was found that the average fibre length within the final composites increased from 159 μm ("classical" extrusion compounding followed by injection moulding) to 658 μm by applying this long fibre injection moulding technology. As a result, around 20% increase was found in tensile and flexural strength of the long basalt fibre reinforced PLA composites compared to the composites with the same fibre ratio but with lower average fibre length, while the most significant improvement was found in the three times higher impact strength. Finally, a review was published recently according to basalt fibre composites including biodegradable matrix composites.[30]

As it was demonstrated, basalt is an excellent reinforcement for PLA and even injection moulded, basalt fibre reinforced PLA parts with high mechanical properties can be made despite of the typically significant fibre breakage taking place during processing. However, to be able to use and design basalt fibre reinforced PLA composites in engineering applications, its long-term behaviour, especially its creep

behaviour needs to be investigated, since thermoplastic polymer based composites are designed not to maximum allowable stress, but to maximum allowable strain. Bakonyi et al.[31-33] extensively researched the creep of glass fibre reinforced Polypropylene (PP) and found that based on the temperature-time and load-time superposition principle, long-term creep curves (mastercurves) could be constructed from short-term creep measurements. In a recent publication[34] the creep of PLA/bamboo fibre compression moulded composites was investigated by using temperature-time superposition principle. However, the number of these papers is still very limited, despite of the interest of reinforced PLA composites in structural applications.

Although the creep of ordinary, petrol based polymers and their composites was extensively investigated, but according to our best knowledge, the number papers dealing with reinforced PLA is very limited, moreover there is not a single paper dealing with the long-term behaviour of basalt fibre reinforced, injection moulded PLA composites. Accordingly in our work, basalt fibre reinforced PLA composites were prepared by using extrusion compounding and the long-term creep behaviour of the final injection moulded composites with different fibre ratio was investigated by using short-term creep tests and load-time superposition principle.

2. Experimental

2.1. Materials

Injection moulding grade PLA type 3052D from NatureWorks (Minnetonka, MN, USA) was used for the research with a D-Lactide content of around 4%. 3052D PLA has a density of 1.24 g/cm^3, a glass transition temperature range of 55-60°C, a melting temperature range of 145-160°C and a melt flow index of 14 g/10min (at 210°C, with 2.16 kg load). Chopped basalt fibres with an initial fibre length of 10 mm

was purchased from Kameny Vek. The average diameter of the fibres was 13 μm and had a silane treatment under trade name KV-12 suitable for polyesters.

2.2. Material preparation and processing

PLA was dried at 120°C for 6 hours prior to processing to remove as much residual moisture as possible to avoid hydrolitical degradation. Even though basalt fibres have no hydrophilic character, they were also dried along with the PLA to remove any residual moisture from the surface of the fibres. PLA based composites with a nominal basalt fibre content of 5, 10, 20, 30 wt% were prepared by using chopped (10 mm) basalt fibres and the conventional dry mixing, extrusion, pelletizing and injection moulding method. The extruder used was a LabTech Scientific twin screw extruder (screw diameter = 26 mm, L/D = 40) with a temperature profile of 175-180-185-190°C (from the hopper to the die) and a screw rotational speed of 10 rpm. All pellets were annealed prior to injection moulding at 120°C for 2 hours to avoid pellet sticking to the screw during injection moulding caused by cold crystallisation reported in our previous research.[35] Finally, the basalt fibre reinforced PLA pellets were injection moulded with an Arburg Allrounder 370S 700-290 injection moulding machine equipped with a 30 mm diameter, L/D = 25 screw. An injection rate of 50 cm^3/s, holding pressure of 600 bars, holding time of 20 sec, residual cooling time of 40 sec, melt and mould temperature of 190°C and 20°C were used. Based on EN ISO standard number 527-2 dumbbell specimens type 1A with 4x10 mm cross-section (172 mm in total length, 80 mm in the length of 4x10 mm cross-section) were injection moulded and used for the investigations.

2.3. Methods

Differential Scanning Calorimetry measurements were performed on a TA Instruments Q2000 type calorimeter (New Castle, USA) by using 3-6 mg of samples taken from the middle of the cross-section of the injection moulded specimens. Since a skin/core structure develops during injection moulding, where

in the skin layer lower, but in the core layer higher crystalline ratio develops due to the different cooling rates, thus in this case, the maximum crystallinity of the given specimen could be determined by taking the calorimetry samples from the middle of the cross-section. The samples were tested in non-isothermal mode (heat/cool/heat) from 0 to 200°C at a heating/cooling rate of 5°C/min to determine glass transition temperature (T_g), cold crystallisation temperature (T_{cc}), enthalpy of cold-crystallisation (ΔH_{cc}), melting temperature (T_m), and enthalpy of fusion (ΔH_m). Crystallinity was calculated from the first heating scan of the injection moulded specimens by using Equation (1):

$$X = \frac{\Delta H_m - \Delta H_{cc}}{\Delta H_f \cdot (1-\alpha)} \cdot 100 ,\tag{1}$$

where X [%] is the calculated crystallinity, ΔH_m [J/g] and ΔH_{cc} [J/g] is the enthalpy of fusion and the enthalpy of cold-crystallisation respectively, ΔH_f [J/g] is the enthalpy of fusion for 100% crystalline PLA (93.0 J/g[36]) and α [-] is the mass fraction of the basalt fibres.

After calcinating the samples (at 700°C for one hour) taken from the middle of the injection moulded specimens, the actual fibre content was determined by analysing the weight of the residual compared to the weight of the sample prior to calcination as well as the fibre length distribution was measured determining the length of the fibres by using optical microscopy (type Olympus BX 51M). 1000 fibre lengths were determined for each sample to characterise distribution.

Scanning Electron Microscopy (SEM) was performed by using a Jeol JSM 6380LA type electron microscope to investigate the quality of adhesion between matrix and reinforcement. The fracture surfaces of the tensile specimens were used for the observations. Au/Pd alloy was sputtered onto the surface prior to observation to avoid electrostatic charging.

Finally, creep tests were performed according to EN ISO 899-2 standard by using a Zwick Z250 universal testing machine. The force and strain (nominal extension) was determined by a Zwick BZ 020/TN2S load cell, and by the movement of the cross-head (the change in distance between the grips)

respectively. The injection moulded samples were used without any further processing or machining, thus the creep of the given sample also represents its skin/core structure developed during processing. First, the tensile strength of each composite was determined by using force controlled tensile testing. Only for the tensile tests, strain was not only determined by the movement of the cross-head, but also more precisely by using an extensometer as a verification. A load rate of 20 N/s was used and 20 specimens were tested. Afterwards, 10, 20, 30, 40, 50, 60, 70, 80 and 90% of the determined maximum force value was used as static loading force for the creep tests. These are named as load "levels" (for instance 30% load level) since it is a dimensionless quantity. 20 N/s load rate was applied until the force reached the given static loading level and kept it for one hour. Two specimens were used for each loading level if the specimens did not break until the one hour creep test, and 6 specimens were used if they were broken during the creep test. All of the measurements were performed at room temperature (23 ± 1°C) and at a relative humidity of 50 ± 10%. Finally, by using the load-time equivalence principle, master curves were constructed. Since every mastercurve is related to a certain load level, thus this desired value must be selected first, namely, in our case 50% of load level was selected. Afterwards, the single time-strain creep curve in logarithmic scale related to the selected load level was depicted in a diagram and the other curves with higher loading levels were fitted to the original curve by shifting in the time-scale. For comparison, mastercurves were also constructed by modifying the creep strain data calculated from the cross-head movement with the strain data obtained during the tensile tests using extensometer. The modification was performed based on the ratio of the strain values measured by the two different method.

3. Results and discussion

First, the DSC measurement of the basalt fibre reinforced PLA composites and the pristine PLA was performed in order to analyse the possible nucleating ability of basalt fibres on PLA and thus the crystallinity of the injection moulded specimens. Although PLA is a semi-crystalline thermoplastic

material, but unfortunately, it has very slow crystallization kinetics, meaning that during injection moulding usually only a few percent of crystallinity develops due to the high cooling rate. Nucleating agents can be used for enhancing crystallization, but it is still challenging to develop high or even the possible maximum crystallinity of around 40-50% during processing.[37] According to the basalt fibre reinforced PLA samples, the first heating scan was analysed and the thermal history was not erased, thus the crystallinity values represent the crystallinity of the injection moulded specimens (Table 1).

Material	ΔH_{cc}/J g^{-1}	ΔH_m/J g^{-1}	X/%	T_g/°C	T_{cc}/°C	T_m/°C
PLA	28.64	29.31	0.7	60.9	106.5	147.3 and 154.7
PLA+5wt% basalt fibre	27.96	28.67	0.8	61.6	102.3	146.7 and 154.8
PLA+10wt% basalt fibre	21.13	26.79	6.8	62.3	102.5	146.9 and 154.9
PLA+20wt% basalt fibre	21.16	26.39	7.0	61.9	103.6	147,1 and 155.1
PLA+30wt% basalt fibre	15.35	19.99	7.1	63.5	104.0	147.2 and 155.0

Table 1. DSC data of the basalt fibre reinforced PLA composites and the pristine PLA obtained from the first heating scan

As it can be seen, the addition of basalt fibres to PLA did not significantly modify the transition temperatures, moreover and most importantly it also had only low effect on the crystallinity values. Although by increasing basalt fibre content crystallinity increased, thus basalt fibres had nucleating ability, probably by developing a trans-crystalline structure around the fibres.[38] However, since a PLA with relatively high D-Lactide content (4%) was used, which is rather difficult to crystallize compared to lower D-Lactide content PLA grades, as a result, only low crystallinity of 7.1% was reached even when 30wt% basalt fibres were added to PLA.

In the next step the real basalt fibre content in the composites (Fig. 1) as well as the distribution of fibre lengths (Fig. 2) was investigated.
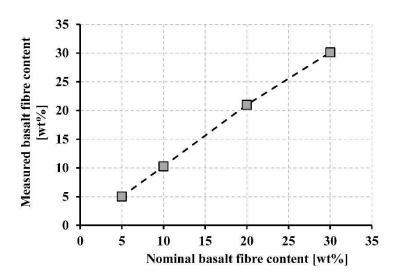
Fig. 1. Measured (real) fibre content in the function of nominal fibre content
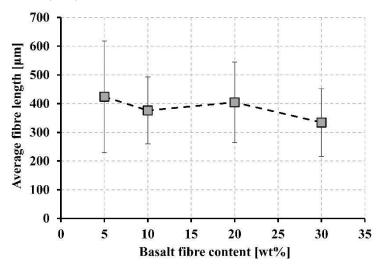

Fig. 2. Average fibre length as a function of fibre content

There was only minor variance found between the nominal and the measured real basalt fibre content of the composites meaning that the technology used to produce the composites was adequately precise. Regarding to the fibre lengths, it can be observed that, the average basalt fibre length was almost independent from the basalt fibre content within the investigated 5-30wt% basalt fibre content range.

Although there was no significant statistical difference found between the average fibre length of all of the composites, namely, 424 ± 194 μm, 376 ± 117 μm, 404 ± 140 μm and 334 ± 118 μm for the 5, 10, 20 and 30wt% basalt fibre composites respectively, but if the whole distribution is taken into consideration (Fig. 3), it is visible that the amount of longer fibres decreased while the amount of shorter fibres increased with increasing basalt fibre content. This could be explained by the increasing fibre-fibre friction during processing with the increasing fibre content.

Fig. 3. Fibre distribution of 5wt% (a), 10wt% (b), 20wt% (c) and 30wt% (d) basalt fibre content PLA composite

After determining the real fibre content and fibre length distribution of specimens, their fracture surface was also investigated by scanning electron microscopy to qualify the adhesion between the phases (Fig. 4).
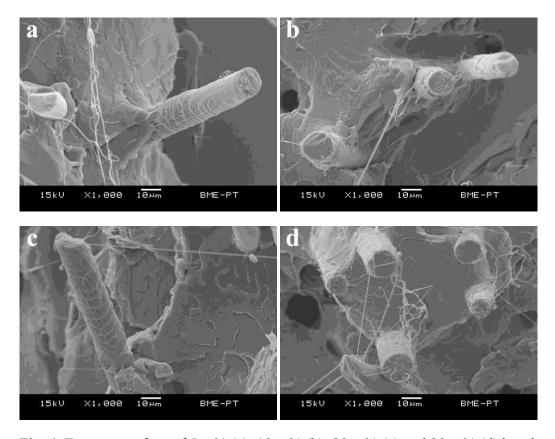
Fig. 4. Fracture surface of 5wt% (a), 10wt% (b), 20wt% (c) and 30wt% (d) basalt fibre content PLA composite

As it is visible, there was strong adhesion found for every compound, which is manifested in the PLA layer that developed on the surface of the basalt fibres as well as in the absence of any gap between the root of the fibres and the matrix. On the other hand, some longer basalt fibres pointing out from the fracture surface suggests that some of the fibres got pulled out. Moreover, interestingly, some of the possibly pulled-out fibres had a periodic band shaped PLA layer along the length of the fibres (Fig. 4/a and /c) which suggests the failure of the matrix by intensive shearing action during the tensile testing. The strong adhesion demonstrated on the SEM images was naturally also observable in the tensile properties of

the composites (Table 2), which was determined to use this maximum force at break value as a point of reference for applying various static loading levels during creep tests.

Material	Tensile strength/MPa	Maximum force at break/N	Strain at break/% (cross-head displacement)	Strain at break/% (extensometer)
PLA	68.9 ± 1.1	2758 ± 46	3.49 ± 0.12	3.26 ± 0.43
PLA+5wt% basalt fibre	73.0 ± 2.0	2920 ± 79	3.05 ± 0.48	2.97 ± 0.31
PLA+10wt% basalt fibre	78.9 ± 0.8	3154 ± 34	2.71 ± 0.34	2.58 ± 0.29
PLA+20wt% basalt fibre	97.7 ± 3.0	3906 ± 120	2.22 ± 0.06	1.94 ± 0.02
PLA+30wt% basalt fibre	106.5 ± 2.4	4260 ± 96	2.01 ± 0.10	1.64 ± 0.14

Table 2. Tensile properties of the basalt fibre reinforced PLA compounds and the pure PLA

Both tensile strength (68.9 MPa + 1.2804 MPa/wt%, R^2=0.98) and strain at break (3.49% - 0.056%/wt%, R^2=0.91 for cross-head displacement and 3.26% - 0.058%/wt%, R^2=0.97 for extensometer) was found to increase and decrease linearly with increasing basalt fibre content in the investigated 0-30wt% basalt fibre range respectively. According to the strain values, there was no statistically significant difference found between the strain of PLA and 5wt% basalt fibre reinforced PLA measured by the two different methods (cross-head displacement and extensometer), On the other hand there was minor difference between the strain of 10wt%, while there was even statistically significant difference between the strain of 20wt% and 30wt% basalt fibre reinforced PLA measured by the two different methods. For the creep tests, the cross-head displacement was used to calculate strain, while for the mastercurves construction, the more precise extensometer strain data obtained from the tensile tests is also taken into account. From the tensile data, 10, 20, 30, 40, 50, 60, 70, 80 and 90% of the determined maximum force at break values were used as a static loading levels for the creep tests. First, the creep behaviour of pure PLA was analysed (Fig. 5).
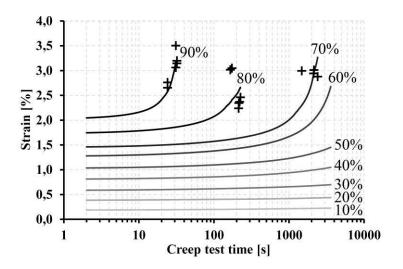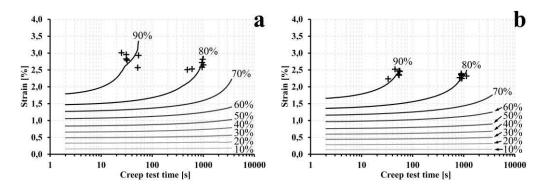
Fig. 5. Creep strain of pure PLA at various static loading levels. The curves are averaged creep curves, while the cross means the breakage of the single specimens

Naturally, the higher the loading level was applied, the higher the strain was measured, moreover, the PLA specimens did not break within the one hour creep test until 70% of the maximum force at break was applied as static loading level. In case of 5wt% basalt fibre reinforcement (Fig. 6/a), the strain of the specimens decreased for the same static loading level, which corresponds to increased creep resistance, meaning that more time was needed to reach the same deformation compared to pure PLA specimens.
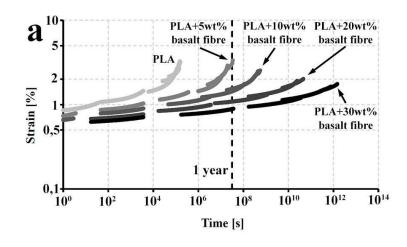
Fig. 6. Creep strain of 5wt% (a), 10wt% (b), 20wt% (c) and 30wt% (d) basalt fibre reinforced PLA at various static loading levels. The curves are averaged creep curves, while the cross means the breakage of the single specimens

Nevertheless, basalt fibres also made the composites more brittle, resulting in decreased maximum strain at break where creep leads to failure, but, on the whole, the creep retarding effect of basalt fibres was still higher than its embrittlement effect, what makes the usage of basalt fibres useful for mechanically loaded long term applications. The same trend could be observed when 10wt% (Fig. 6/b), 20wt% (Fig. 6/c) or 30wt% (Fig. 6/d) basalt fibre reinforcement was used. Finally, creep master curves were constructed from the single creep curves in case of 50% loading level by applying the load-time equivalence principle (Fig. 7).
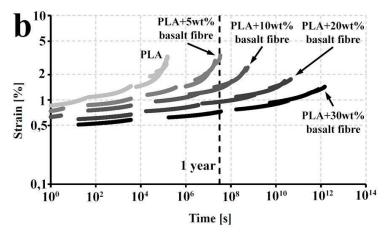
Fig. 7. Creep mastercurves for pure PLA and 5wt%, 10wt%, 20wt%, 30wt% basalt fibre reinforced PLA in case of 50% loading level constructed by using the creep strain data from cross-head displacement (a) and from modified creep strain data obtained by extensometer measurements (b)

As it was discussed previously, it is also visible and easily observable in the master curves that by increasing the basalt fibre content, the strain at break naturally decreases, thus failure occurs at lower strain values, at the same time, the creep resistance increases even more, which results in increased time to failure. Although crystalline structure could also reduce creep, but in this case, the reduced deformation can be

almost entirely related to basalt fibre content, since it was proved previously that these fibres had only negligible effect on the crystallinity of the PLA grade used in this study. It can also be observed that despite of the increasing fibre length reduction experienced with increasing fibre content as proved previously, there was still remarkable improvement found in creep resistance with more and more increasing fibre content in the investigated 0-30wt% fibre content range, which could be related to the strong fibre-matrix adhesion as well as to the increased fibre content naturally. For comparison, mastercurves were also constructed by modifying the creep strain data (obtained from cross-head displacement) by the tensile test strain results obtained by using extensometer. Since there was no significant statistical difference between the strain of PLA and 5wt% basalt fibre reinforced PLA measured by the two different methods (Table 2), thus only the strain of 10wt%, 20wt% and 30wt% basalt fibre reinforced PLA was modified (Fig. 7/b). As it is visible, the mastercurves of 10wt%, 20wt% and 30wt% basalt fibre reinforced PLA shifted to lower strain values, however, this decrease was rather minor. Nevertheless, much higher difference is expected between the strain measured by using the two different methods in case of highly reinforced, thermoset materials.

Finally, the creep strain time (at failure) estimation obtained from the mastercurves was also plotted against basalt fibre content (Fig. 8) to be able to investigate the effect of basalt fibre content directly.
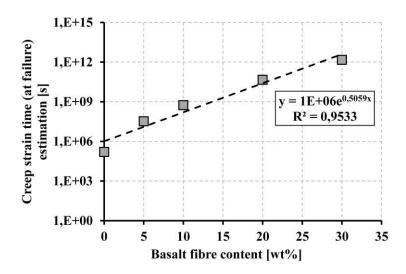
Fig. 8. Creep strain time (to failure) estimation as a function of basalt fibre content in case of 50% loading level

As it is visible, the creep strain (at failure) estimation obtained from the master-curves could be very well fitted by an exponential equation with the basalt fibre content as variable in the investigated 0-30wt% basalt content range. All these results demonstrate that the basalt fibre reinforced PLA based composites could even be used in long-term constantly loaded structural or engineering applications.

4. Conclusion

In our research the creep of short (chopped) basalt fibre reinforced Poly(Lactic Acid) (PLA) composites was investigated. 5, 10, 20 and 30wt% short basalt fibre reinforced composites were prepared by twin-screw extrusion followed by injection moulding. Differential Scanning Calorimetry (DSC) measurements revealed that the selected basalt fibres had nucleating effect on PLA used for this study, accordingly, the crystallinity of injection moulded PLA of 0.7% was increased up to 7.1% by incorporating 30wt% of basalt fibres. However, the low increase in crystallinity could be explained by the rather high D-Lactide content (4%) of the PLA used, which is difficult to crystallize compared to a PLA with lower D-

Lactide content. The real basalt fibre content of the composites was measured and it was in good accordance with the nominal fibre content. According to the fibre distribution, there was no significant statistical difference found between the average fibre length of 5wt%, 10wt%, 20wt% and 30wt% basalt fibre composites, but if the whole distribution is taken into consideration it was visible that the amount of longer fibres decreased while the amount of shorter fibres increased with increasing fibre content. Scanning Electron Microscopy (SEM) revealed that there was strong adhesion between the fibre and the matrix, at the same time, some of the possibly pulled-out fibres had a periodic band shaped PLA layer along the length of the fibres which suggests the failure of the matrix by intensive shearing action. Prior to creep measurements, the tensile strength of the basalt fibre reinforced composites was determined, to be able to use 10, 20, 30, …, 90% of the tensile strength of the composites as a static creep loading force. Creep mastercurves were constructed using the short-term single creep curves obtained by applying various static creep loading forces determined previously and the load-time equivalence principle. It was demonstrated that the basalt fibres as reinforcements can effectively reduce the creep strain of the composites and despite of the fibre length reduction demonstrated previously, there was still significant creep resistance improvement found with more and more increasing fibre content due to strong fibre-matrix adhesion. Finally, all these result demonstrate, that by using the conventional twin-screw extrusion and injection moulding techniques, the short basalt fibre reinforced, injection moulded PLA could even be used in long-term constantly loaded structural or engineering applications.

Acknowledgement

References

1   Flieger M, Kantorová M, Prell A, et al. Biodegradable plastics from renewable resources. *Folia Microbiol* 2003; 48: 27-44.

2   Lim LT, Auras R and Rubino M. Processing technologies for poly(lactic acid). *Prog Polym Sci* 2008; 33: 820-852.

3   Mihai M, Huneault MA and Favis BD. Crystallinity Development in Cellular Poly(lactic acid) in the Presence of Supercritical Carbon Dioxide. *J Appl Polym Sci* 2009; 113: 2920-2932.

4   Imre B, Renner K and Pukánszky B. Interactions, structure and properties in poly(lactic acid)/thermoplastic polymer blends. *Express Polym Lett* 2014; 8: 2-14.

5   Karger-Kocsis J and Kéki S. Biodegradable polyester-based shape memory polymers: Concepts of (supra)molecular architecturing. *Express Polym Lett* 2014; 8: 397-412.

6   Yu L, Dean K and Li L. Polymer blends and composites from renewable resources. *Prog Polym Sci* 2006; 31: 576-602.

7   Iwatake A, Nogi M and Yano H. Cellulose nanofiber-reinforced polylactic acid. *Compos Sci Technol* 2008; 68: 2103-2106.

8   Suryanegara L, Nakagaito AN and Yano H. The effect of crystallization of PLA on the thermal and mechanical properties of microfibrillated cellulose-reinforced PLA composites. *Compos Sci Technol* 2009; 69: 1187-1192.

9   Oksman K, Skrifvars M and Selin JF. Natural fibres as reinforced in polylactic acid (PLA) composites. *Compos Sci Technol* 2003; 63: 1317-1324.

10   Ganster J, Fink HP and Pinnow M. High-tenacity man-made cellulose fibre reinforced thermoplastics – Injection moulding compounds with polypropylene and alternative matrices. *Compos Part A-Appl S* 2006; 37: 1796-1804.

11 Plackett D, Andersen TL, Pedersen WB, et al. Biodegradable composites based on l-polylactide and jute fibres. *Compos Sci Technol* 2003; **63:** 1287-1296.

12 Bodros E, Pillin I, Montrelay N, et al. Could biopolymers reinforced by randomly scattered flax fibre be used in structural applications? *Compos Sci Technol* 2007; 67: 462-470.

13 Bax B and Müssig J. Impact and tensile properties of PLA/Cordenka and PLA/flax composites. *Compos Sci Technol* 2008; 68: 1601-1607.

14 Huda MS, Drzal LT, Mohanty AK, et al. Chopped glass and recycled newspaper as reinforcement fibers in injection molded poly(lactic acid) (PLA) composites: A comparative study. *Compos Sci Technol* 2006; 66: 1813-1824.

15 Kimble LD, Bhattacharrya D and Fakirov S. Biodegradable microfibrillar polymer-polymer composites from poly(L-lactic acid)/poly(glycolic acid). *Express Polym Lett* 2015; 9: 300-307.

16 Kowalczyk M, Piorkowska E, Kulpinski P, et al. Mechanical and thermal properties of PLA composites with cellulose nanofibers and standard size fibers. *Compos Part A-Appl S* 2011; 42: 1509-1514.

17 Cho SY, Park HH, Yun YS, et al. Cellulose nanowhisker-incorporated poly(lactic acid) composites for high thermal stability. *Fiber Polym* 2013; 14: 1001-1005.

18 Kabir MM, Wang H, Lau KT, et al. Effects of chemical treatments on hemp fibre structure. *Appl Surf Sci* 2013; 276: 13-23.

19 Czigány T, Deák T and Tamás P. Discontinuous basalt and glass fiber reinforced PP composites from textile prefabricates: effects of interfacial modification on the mechanical performance. *Compos Interface* 2008, 15: 697-707.

20 Wei B, Cao H and Song S. Tensile behavior contrast of basalt and glass fibers after chemical treatment. *Mater Design* 2010; 31: 4244-4250.

21 Wei B, Cao H and Song S. Environmental resistance and mechanical performance of basalt and glass fibers. *Mat Sci Eng A-Struct* 2010; 527: 4708-4715.

22 Gur'ev VV, Neproshin EI and Mostovoi GE. The effect of basalt fiber production technology on mechanical properties of fiber. *Glass Ceram+* 2011; 58: 62-65.

23 Xi C, Li Y and Gu N. A novel basalt fiber reinforced polylactic acid composite for hard tissue repair. *Biomed Mater* 2010; 5: 1-8.

24 Liu T, Yu F, Yu X, et al. Basalt fiber reinforced and elastomer toughened polylactide composites: Mechanical properties, rheology, crystallization and morphology. *J Appl Polym Sci* 2012; 125: 1292-1301.

25 Kurniawan D, Kim BS, Lee HY, et al. Atmospheric pressure glow discharge plasma polymerization for surface treatment on sized basalt fiber/polylactic acid composites. *Compos Part B-Eng* 2012; 43: 1010-1014.

26 Tábi T, Tamás P and Kovács JG. Chopped basalt fibres: A new perspective in reinforcing poly(lactic acid) to produce injection moulded engineering composites from renewable and natural resources. *Express Polym Lett* 2013; 7: 107-119.

27 Tábi T, Égerházi AZ, Tamás P, et al. Investigation of injection moulded poly(lactic acid) reinforced with long basalt fibres. *Compos Part A-Appl S* 2014; 64: 99-106.

28 Wittek T and Tanimoto T. Mechanical properties and fire retardancy of bidirectional reinforced composite based on biodegradable starch resin and basalt fibres. *Express Polym Lett* 2008; 2: 810-822.

29 Peng Y, Reitz L, Horan C, et al. Manufacture and biodegradation of wheat gluten/basalt composite material. *J Polym Environ* 2006; 14: 1-7.

30 Fiore V, Scalici T, Di Bella G, et al. A review on basalt fibre and its composites. *Compos Part B-Eng* 2015; 74: 74-94.

31 Vas LM and Bakonyi P. Creep failure strain estimation of glass fibre/polypropylene composites based on short-term tests and Weibull characterisation. *J Reinf Plast Comp* 2013; 32: 34-41.

32 Bakonyi P and Vas LM. Analysis of the creep behaviour of polypropylene and glass fiber reinforced polypropylene composites. *Mater Sci Forum* 2013; 729: 302-307.

33 Vas LM and Bakonyi P. Estimating the creep strain to failure of PP and different load levels based on short term tests and Weibull characterization. *Express Polym Lett* 2012; 6: 987-996.

34 Yang TC, Wu TL, Hung KC, et al. Mechanical properties and extended creep behavior of bamboo fiber reinforced recycled poly(lactic acid) composites using the time–temperature superposition principle. *Constr Build Mater* 2015; 93: 558-563.

35 Tábi T, Sajó IE, Szabó F, et al. Crystalline structure of annealed polylactic acid and its relation to processing. *Express Polym Lett* 2010; 4: 659-668.

36 Battegazzore D, Bocchini S and Frache A. Crystallisation kinetics of poly(lactic acid)-talc composites. *Express Polym Lett* 2011; 5: 849-858.

37 Tábi T, Kovács NK, Sajó IE, et al. Comparison of thermal, mechanical and thermomechanical properties of poly(lactic acid) injection-molded into epoxy-based Rapid Prototyped (PolyJet) and conventional steel mold. *J Therm Anal Calorim* 2016; 123: 349-361.

38 Tao L, Xuejiang Y, Fengmei Y, et al. Isothermal crystallization kinetics of fiber/polylactic acid composites and morphology. *Polym-Plast Technol* 2012; 51: 597-604.